Discrete Light Source Estimation from Light Probes for Photorealistic Rendering

Farshad Einabadi
einabadi@intel-vci.uni-saarland.de
Intel Visual Computing Institute
Saarbrücken, Germany
Oliver Grau
oliver.grau@intel.com
Intel Corporation

Abstract

This contribution describes a new technique for estimation of discrete spot light sources. The method uses a consumer grade DSLR camera equipped with a fisheye lens to capture light probe images registered to the scene. From these probe images the geometric and radiometric properties of the dominant light sources in the scene are estimated. The first step is a robust approach to identify light sources in the light probes and to find exact positions by triangulation. Then the light direction and radiometric fall-off properties are formulated and estimated in a least square minimization approach.

The new method shows quantitatively accurate estimates compared to ground truth measurements. We also tested the results in an augmented reality context by rendering a synthetic reference object scanned with a 3D scanner into an image of the scene with the estimated light properties. The rendered images give photorealistic results of the shadow and shading compared to images of the real reference object.

1 Introduction

The interaction between light source, surface and an observing camera is a fundamental relation used in many computer vision approaches, like in the early work on shape-from-shading from Horn [11]. This work made a number of simplifying assumptions about the light source, the scene and the camera. However, it is able to estimate one dominant explicit discrete light model (far directional) under these assumptions.

Applications like rendering of images using computer graphics methods are usually requiring more sophisticated light models to give better control. Complex scenes in computer generated images are requiring very differentiated light models to give a realistic rendering of the scene. That usually includes a high number of (virtual) light sources to model a scene to reproduce accurate shadows and shadings. In particular in the production of visual effects for movies and TV the real scene lighting needs to be captured very accurately to give a realistic rendering of virtual objects into that scene. In this context the light modeling is usually done manually by skilled artists in a time consuming process.

Image-based light capture, as pioneered by Debevec [6] was introduced as a fast method to capture the lighting situation of a real scene. It requires a rendering method capable of using the captured light probes, usually a ray tracing or global illumination renderer. Furthermore, the method is constrained to scenes with small extend; strictly speaking the light probe

Pages 43.1-43.10
DOI: https://dx.doi.org/10.5244/C.29.43

illumination model is only valid for one point of the scene: the center or nodal point of the light capture device. Having said that, these approaches tend to produce photorealistic results when the above conditions are met. These models basically contain *all* the lighting information of the scene for that certain point. There are a couple of efforts for sampling important areas of these light probes and modeling them with many point light sources [5, 7, 14]. This idea, although makes the rendering faster and produces visually comparable results to using all the information in light probes, is not modeling the actual sources, and hence suffers from the same mentioned problem.

The approach presented in this paper aims to estimate discrete spot light source models from a number of image light probes, captured at different positions in the real scene. From this information we estimate the position of a number of light sources, their orientations, relative intensities and radiometric fall-off characteristics. In contrast to image-based lighting, once the sources are modeled separately, they can be used for augmenting assets in different positions flawlessly.

1.1 Related Work

Estimating discrete light sources from images, although desirable, with high precision as needed for photorealistic rendering doesn't have much prior work. In the most simplified case, light sources are only modeled with an incident direction (distant light source assumption) [15, 20]. However, for a more accurate estimation of the light geometric properties, point [8, 9, 17, 21] or area light [18] sources are taken into account. In these cases, the type of light source must be known beforehand. To cope with this limitation, Zhou and Kambhamettu [22] and Takai *et al*. [19] assume more generic light source models and estimate their parameters accordingly. Here an interface to the renderer is required to transform parameters of the chosen general model to the available light source types in the renderer.

Regarding the capture setups, a common approach is to use reflective objects of known geometries like mirror spheres which can be used for finding geometric properties of the light sources *e.g*. their directions and/or 3D positions [12, 17]. Weber and Cipolla [21] use a calibration cube with Lambertian reflectance. However, using a probing object generally implies knowing its geometry and the exact material model in advance. Ackermann *et al*. have recently proposed to directly triangulate the visible light sources in captured images for the geometric calibration [4]. Although, due to the limits of their setup, they had to use mirror spheres for registration of the probing camera itself.

Park *et al*. [16] investigated the problem of image-based geometric and radiometric calibration of non-isotropic near point light sources based on shading cues on a probing plane (here whiteboard). In addition to the 3D position of the point source, its dominant direction and the intensity fall-off parameters are estimated. However, due to their setup and the inherent limited field of view of the normal lenses employed, estimated fall-off parameters are valid for a limited range.

In our proposed setup we use a consumer grade DSLR camera equipped with a fisheye lens to capture light probes from a few different positions in the studio environment to estimate geometric and radiometric properties of studio spot lamps including the 3D position, dominant direction (light axis), relative intensity and the intensity fall-off parameters. In contrast to the above mentioned methods, there are a number of advantages in our approach. First, the probing camera is registered using a multi-camera setup which requires the minimum amendments to the studio. Second, we are not limited to any specific probing object since the properties of each light are estimated based on processing the probe images. In addition,

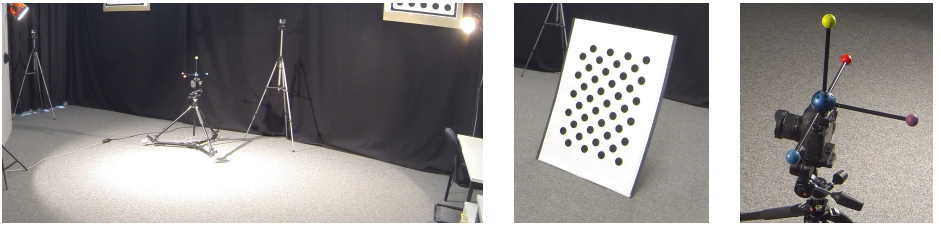

(a) (b) (c)

Figure 1: (a) Multi-camera setup from one of the witness camera views (cropped): the other two witness cameras and two lamps are visible; fisheye probing camera in the middle (b) Calibration pattern used for registering the witness cameras (c) Attached calibration rig for registering the probing camera

since the probing camera can move freely in the area of interest, there are no limits in terms of the covered space. Large field of view of the fisheye lens is also beneficial in this matter.

In the following, our proposed approach is discussed in detail in Section 2. Section 3 covers the experiments, results and the relevant discussions. The paper ends with conclusions and possible future directions in Section 4.

2 Discrete Light Source Estimation

Our proposed method is based on directly processing the linear light probes taken with a fisheye camera system. The probing camera is registered with a few witness cameras, a planar calibration pattern, and a calibration rig attached to it (Figure 1). Having a minimum number of 5 registered light probes where each individual light is visible in them, we aim for estimation of its geometric and radiometric properties. First, 3D position vector of each lamp is computed based on the triangulation of corresponding rays to 2D position of the existing bright light blobs in the segmented probes. Then the brightness of these blobs are used in a proposed non-linear least square optimization scheme to find the dominant directions, relative intensities and fall-off parameters of the lamps. Observations are the blobs' brightness values and we use a quadratic fall-off function by minimizing the squared errors to find the corresponding maximum intensities and dominant directions. The rest of this section covers these three steps separately.

2.1 Calibration and Registration of Cameras

We propose a two-step calibration and registration approach. In the first step, a planar asymmetric calibration pattern (Figure 1) is used for simultaneous calibration of the intrinsics and the pose of all the witness cameras and the principal camera using the bundle adjustment module from R3DR [3]. To minimize the calibration error, the pattern must be captured in different positions and orientations. The pattern can be easily detected using OpenCV [2] and the found features are fed into the bundle adjustment module. In the next step, parameters of witness cameras are kept fixed and the probing camera is registered in the same coordinate system by extraction of the four color features of the attached calibration rig (Figure 1) and the same bundle adjustment module.

Inputs:
A couple of registered light probe images
Intrinsic calibration parameters of the probing camera
Output:
3D position vectors of light sources
Steps:
Detect light blobs in all probe images
Match light blobs to their corresponding light source
For all detected light sources
Shoot rays from corresponding light blobs
Triangulate computed rays
Return the estimated 3D position of the light source

Figure 2: Pseudocode for estimating positions of the light sources

Regarding the fisheye camera-lens system, the basic radially symmetric polynomial model of Kannala and Brandt [13] is employed to calibrate its geometric projection.

2.2 Position Estimation

To estimate the 3D position vectors of the light sources, one needs to shoot rays from every detected light blob in all probe images and triangulate the corresponding rays from at least two probe positions for each source. Figure 2 shows the overview of the required steps.

Since the light sources are by far brighter than the studio environment, the corresponding light blobs are easily detected by thresholding the luminance values in the probe images. The area of the detected blobs are also checked to be bigger than a threshold to avoid noisy pixels (see Figure 3). For the matching step, considering the light blobs detected in all probe images altogether, the first corresponding ray to the blobs is assigned to the first light source. Then based on a distance threshold, each subsequent ray is checked to be assigned to one of the existing light sources or create a new light source. Finally, a linear system of equations is made for each light source and the corresponding rays are triangulated with the least square method. For a review on triangulation approaches, interested reader can refer to [10].

2.3 Dominant Direction and Fall-off Curve Estimation

In terms of the radiometric characteristics, we assume spot light sources have a dominant direction where the intensity fall-off is radially symmetric around it. To find this direction

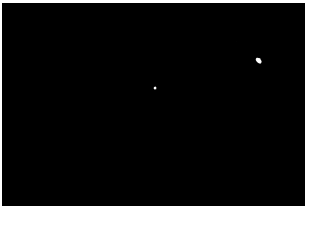

Figure 3: A sample thresholded light probe image

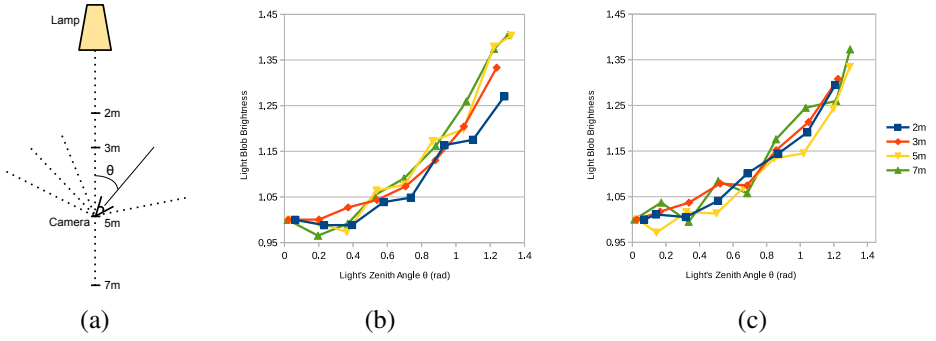

(a) (b) (c)

Figure 4: Radiometric calibration of the probing camera-lens system: (a) sampling process (b), (c) distance-normalized blob brightness values w.r.t. zenith angle θ of the lamp

and the corresponding fall-off parameters, we propose to model the problem as a non-linear least square optimization and solve it with the Levenberg–Marquardt method.

Measured Observations. Observed intensity of a light source at each probe position is considered to be related to the brightness of its corresponding blob in the thresholded probe image. The brightness of each blob is also intuitively defined as summation over its pixel values. However, the probing device must be radiometrically calibrated to find this relation and count for all the present effects of the camera-lens system. This is a one-time procedure which has to be done offline for the chosen probing camera.

For the radiometric calibration of our probing camera, a fixed spot lamp is captured at its dominant direction from different distances and at every distance with varying lens orientations so that the light blobs appear on different areas of the camera's sensor plane (see Figure 4a). Around 70 samples gathered at 4 distances (2m, 3m, 5m, 7m), and at every distance with 16 to 18 lens orientation forming two different paths on the camera's sensor plane starting from its center. Based on this data, we verify that brightness of the light blobs at a fixed lens orientation has quadratic attenuation w.r.t. probing distance. In addition to this, a brightness factor is introduced to model the change in blob brightness values w.r.t. lens orientation. For our camera-lens system, this factor is modeled with $C(\theta) = \alpha\theta^2 + 1$ where C is the brightness factor, θ is the zenith angle of the lamp *i.e.* the angle between the camera optical axis and the camera-lamp vector, and α an equation constant. We estimated $\alpha = 0.20$ through a least square fit to the measured samples. Figure 4 shows the calibration sampling process and the distance-normalized blob brightness values sampled on different areas of the camera's sensor plane.

Least Square Formulation. For a light source j with 3D position L_j, the goal is to find its dominant direction, $\overrightarrow{l_j}$, and parameters of its intensity fall-off function, $I_j(\phi)$, that minimize

$$\sum_{i=0}^{m} \left(I_j(\phi_{ij}) - \frac{B_{ij} \cdot \|P_i - L_j\|^2}{C(\theta)} \right)^2 \tag{1}$$

with m the number of probes where the light source j is visible in them and P_is their corresponding 3D positions. B_{ij} is brightness of light blob j in probe i and the terms $\|P_i - L_j\|^2$ and $C(\theta)$ compensate for its quadratic attenuation w.r.t. probing distance and its brightness factor based on its place on camera's sensor plane, respectively. The angle ϕ_{ij} is also defined

as

$$\phi_{ij} = \angle(\overrightarrow{l_j}, P_i - L_j). \tag{2}$$

In our formulation we assume a quadratic intensity fall-off for spot lights

$$I_j(\phi_{ij}) = k_1 \phi_{ij}^2 + k_2 \tag{3}$$

where the maximum intensity, k_2, happens at the dominant direction $\phi = 0$ and $-k_2/k_1$ is the beam angle. The chosen I_j can model the coarse fall-off characteristics of a real studio spot lamp with a limited number of probe observations. We verify this choice against the linear fall-off curve in the Experiments section.

3 Experiments

To verify the proposed approach, we recorded a real dataset in our studio of a scene (approx. 3x3m) illuminated with two 800W 3200K tungsten halogen lamps with different positions, directions, intensities and beam spreads. The intensities are set using a PC-connected DMX controller and a DMX controlled dimmer kit. Our probing camera is a Canon EOS-5D Mark III with a Walimex Pro 8mm fisheye lens which has 164.5° horizontal field of view (fov). This camera was also used to capture images of a reference object in a separate step with a rectilinear lens at the same color balance settings. Regarding the witness cameras used to register the light probes, 3 GoPro HERO3s at medium field of view setting (80.5° horizontal fov) are fixed around the scene.

Light probes are taken from 18 positions at a fixed height using a moving tripod dolly. At every position, two horizontal probes are captured with opposite viewing directions as an attempt to cover the whole scene from that view point. These probes are roughly captured in the area lit by the lamps. They are taken with the lowest exposure setting on the camera (ISO speed 50, shutter speed 1/8000 sec, aperture size $f/22$) so that the bright areas are not saturated on the sensor plane. High Dynamic Range (HDR) probes are not necessary in this work since only the bright areas of the scene are of interest. In our experiments, we achieved the same estimation results when using HDR probes in comparison to single exposure probes.

In our first experiment to check the stability of the least square minimization method proposed in Subsection 2.3 and verify our choice of the quadratic fall-off curve, we ran the optimization process 1000 times with the following 5 starting values: the maximum intensity $k2$ a positive number, and $k1$ a negative number both in the same order of magnitudes of the observed brightness values; first two elements of the direction vector uniform random samples in $[-1,1]$, and its third element -1. This is due to the fact that the lamps are normally looking down in the studio and if the process starts from -1 it is more likely to converge to a negative value. If the elements of the found solution vector are outside the ranges of interest, it is considered as an invalid solution to our problem *e.g.* in case of negative maximum intensity. Table 1 shows the convergence results for both of the lamps in our dataset. Runtimes are measured using the SciPy implementation under Linux on a Intel Core i7-3770K machine. The results clearly show that although both linear and quadratic fall-off curves apply reasonably well on lamp 2, linear fall-off curve assumption on lamp 1 suffers from instability and larger sum of squared residuals (more than 5 times) in comparison to quadratic curve. In this experiment, only one valid solution was found for each lamp with a certain fall-off assumption over all runs.

#	Fall-off Curve	Residual	No. Steps	Elapsed Time	Valid Solution Found
1	Quadratic	$1.77e-3$	121.61	101.17 ms	99.3%
	Linear	$9.44e-3$	164.99	130.39 ms	75.3%
2	Quadratic	9.50	108.90	91.43 ms	99.7%
	Linear	4.28	93.64	74.56 ms	99.9%

Table 1: Statistics of least square minimization process averaged over 1000 runs

#		Position L (m)	Direction $\overrightarrow{l}$	Intensity k_2	Beam Angle $-k_2/k_1$
1	Estimated	(2.76, 3.75, 1.95)	(-0.8, -0.35, -0.46)	2.75	56.22°
	Measured	(-, -, 1.84)	(-0.80, -0.41, -0.43)	4.0e3 lux	58.0°
	Error	(-, -, 0.11)	3.86°	-	1.78°
2	Estimated	(-1.11, 1.15, 1.78)	(0.47, 0.52, -0.71)	8.98	50.50°
	Measured	(-, -, 1.73)	(0.49, 0.51, -0.71)	1.59e4 lux	50.3°
	Error	(-, -, 0.04)	0.88°	-	0.2°

Table 2: Estimation results for the lamps in our dataset assuming a quadratic fall-off curve

Table 2 shows the estimation results for the two lamps assuming a quadratic fall-off function. Reference values are precisely measured with a laser distance meter and a light meter to our best. In terms of the estimated positions, we can only verify the height of the lamps from floor where the errors (11cm and 4cm) seem acceptable to the scale of our scene. We believe that this triangulation error can be further reduced if more than 3 witness cameras are used so that we get better registrations of probes. Directions and beam angles are also estimated with a small error; however, estimation results of lamp 2 are better. The reason is that lamp 2 has smaller beam angle and lower height which causes the probes to cover its whole beam cone which is not perfectly the case for lamp 1. We only determine relative intensities. For absolute intensities a calibration of the camera is needed. For our lamps, the measured ratio by light meter at 1m distance is $4.0e3/1.59e4 = 0.25$ and the estimated one is $2.75/8.98 = 0.31$.

Furthermore, we use above quantitative estimations of the lamps to render a reference object in our scene from a principal camera's point of view. A plaster fish statue is scanned with a 3D scanner and its model is rendered into the image of an empty table with known 3D geometry without the real fish as the backplate. Shadows of the (virtual) fish on the top surface of the table are generated based on the estimated properties of the above two lamps used in the virtual scene. Intel's Embree [1] is employed for rendering which is a collection of open source high performance ray tracing kernels optimized for Intel's platforms. We use the implemented path tracer method included in the package. Figure 5 shows renders of the fish 3D model side by side to its real appearance at two different positions on the table top about 1m away from each other. One can visually verify the shape, direction and brightness of the rendered shadows. A fixed ambient light is added to the scene to roughly model the reflections from the uncovered studio walls and floor.

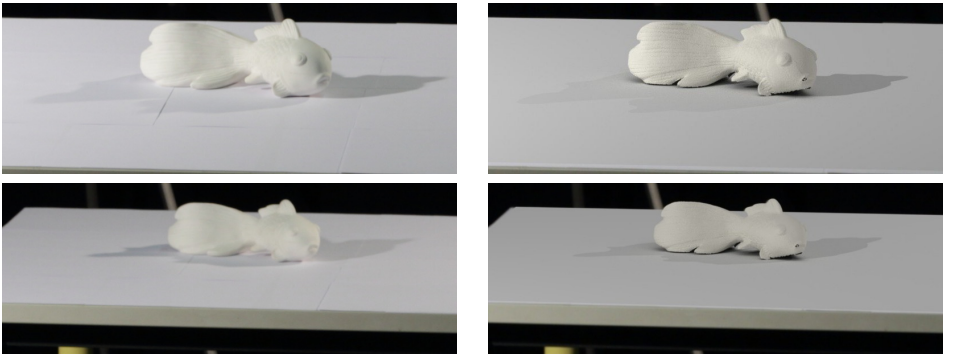

Figure 5: Visual comparison of renders of the reference object (right) to the real ones (left)

4 Conclusion and Future Works

We presented a practical technique to estimate geometric and radiometric properties of real spot light sources. The idea is to probe the environment with a normal fisheye camera from a couple of positions where the probes are registered using a multi-camera system setup. 3D position of sources are estimated through a triangulation process. In addition, a new algorithm proposed to estimate the corresponding light axis, intensity and radiometric fall-off characteristics. We tested our algorithms on real datasets recorded in our studio. The quantitative results are quite accurate. The light positions were estimated within 6% of the real measurements. Errors in the estimated light directions and beam angles are also under 4° and 2°, respectively. In addition, for applications like visual effects and augmented reality, synthetic shadows of scanned objects create very realistic looking results compared to the real reference object.

Future work will be focusing on making the approach more robust and in particular investigate more flexible ways in capturing light probes with fewer samples.

Acknowledgments

This research has received funding from the European Commission's Seventh Framework Programme under grant agreement no 610005 DREAMSPACE.

References

[1] Embree: High performance ray tracing kernels. URL embree.github.io.

[2] Open source computer vision (OpenCV). URL opencv.org.

[3] Robust 3D reconstruction from visual data (R3DR). URL resources.mpi-inf.mpg.de/R3DR/dlm.

[4] Jens Ackermann, Simon Fuhrmann, and Michael Goesele. Geometric point light source calibration. In *Proc. Vision, Modeling, and Visualization*, pages 161–168, 2013.

[5] Sameer Agarwal, Ravi Ramamoorthi, Serge Belongie, and Henrik Wann Jensen. Structured importance sampling of environment maps. In *Proc. ACM SIGGRAPH*, pages 605–612, 2003.

[6] Paul Debevec. Rendering synthetic objects into real scenes: bridging traditional and image-based graphics with global illumination and high dynamic range photography. In *Proc. ACM SIGGRAPH*, page 32, 1998.

[7] Paul Debevec. A median cut algorithm for light probe sampling. In *Proc. ACM SIGGRAPH*, page 33, 2008.

[8] Jan-Michael Frahm, Kevin Koeser, Daniel Grest, and Reinhard Koch. Markerless augmented reality with light source estimation for direct illumination. In *Proc. IEE CVMP*, pages 211–220, 2005.

[9] Kenji Hara, Ko Nishino, and Katsushi Ikeuchi. Light source position and reflectance estimation from a single view without the distant illumination assumption. *IEEE Trans. PAMI*, 27(4):493–505, 2005.

[10] Richard I Hartley and Peter Sturm. Triangulation. *Computer vision and image understanding*, 68(2):146–157, 1997.

[11] Berthold Horn. Obtaining shape from shading information. In Patric Henry Winston, editor, *The psychology of computer vision*, pages 115–155. McGraw-Hill, 1975.

[12] Masayuki Kanbara and Naokazu Yokoya. Real-time estimation of light source environment for photorealistic augmented reality. In *Proc. ICPR*, pages 911–914, 2004.

[13] Juho Kannala and Sami S Brandt. A generic camera model and calibration method for conventional, wide-angle, and fish-eye lenses. *IEEE Trans. PAMI*, 28(8):1335–1340, 2006.

[14] Thomas Kollig and Alexander Keller. Efficient illumination by high dynamic range images. In *Proc. Eurographics Rendering*, pages 45–51, 2003.

[15] Yanli Liu, Xueying Qin, Songhua Xu, Eihachiro Nakamae, and Qunsheng Peng. Light source estimation of outdoor scenes for mixed reality. *The Visual Computer*, 25(5-7): 637–646, 2009.

[16] Jaesik Park, Sudipta N Sinha, Yasuyuki Matsushita, Yu-Wing Tai, and In So Kweon. Calibrating a non-isotropic near point light source using a plane. In *Proc. IEEE CVPR*, pages 2267–2274, 2014.

[17] Mark W. Powell, Sudeep Sarkar, and Dmitry Goldgof. A simple strategy for calibrating the geometry of light sources. *IEEE Trans. PAMI*, 23(9):1022–1027, 2001.

[18] Dirk Schnieders, Kwan-Yee K Wong, and Zhenwen Dai. Polygonal light source estimation. In *Proc. ACCV*, pages 96–107, 2009.

[19] Takeshi Takai, Atsuto Maki, Koichiro Niinuma, and Takashi Matsuyama. Difference sphere: an approach to near light source estimation. *Computer Vision and Image Understanding*, 113(9):966–978, 2009.

[20] Yang Wang and Dimitris Samaras. Estimation of multiple directional light sources for synthesis of augmented reality images. *Graphical Models*, 65(4):185–205, 2003.

[21] Martin Weber and Roberto Cipolla. A practical method for estimation of point light-sources. In *Proc. BMVC*, pages 1–10, 2001.

[22] Wei Zhou and Chandra Kambhamettu. A unified framework for scene illuminant estimation. *Image and Vision Computing*, 26(3):415–429, 2008.